Molecular Modelling of Saccharides, 9[◇]

On the Hydrophobic Characteristics of Cyclodextrins: Computer-Aided Visualization of Molecular Lipophilicity Patterns☆

Frieder W. Lichtenthaler* and Stefan Immel

Institut für Organische Chemie der Technischen Hochschule Darmstadt,
Petersenstraße 22, D-64287 Darmstadt
Telefax: (internat.) +49(0)6151-166674

Received September 21, 1995

Key Words: Cyclodextrins / Molecular geometries / Solution geometries / Molecular lipophilicity patterns / Inclusion complexes

Statistical analysis of the solid-state structures available for the cyclodextrins and their inclusion compounds – 42 for α-CD (**1**), 48 for β-CD (**2**), and 8 for γ-CD (**3**) – revealed their mean molecular geometry parameters to be within normal ranges, such as the intersaccharidic bond angle (φ) and torsion angles Φ and Ψ, or the tilt angle (τ) signifying the inclination of the pyranoid $^4C_1$ chairs toward the macroring perimeter. The mean 2-O···O-3′ distances between adjacent glucose portions decrease in the order α-CD > β-CD > γ-CD from 3.05 to 2.84 Å, allowing more intense 2-O···HO-3′ hydrogen bonding interactions. This reduces the overall flexibility of the macrocycles correspondingly. The intersaccharidic oxygens that without exception point toward the inside of the macrocycles, essentially lie in one plane, deviations from planarity being in the range of only 0.02–0.12 Å. The global molecular shape of **1**–**3** in their various hydrates and inclusion complexes is thus uniformly characterized by essentially unstrained, torus-shaped cones with a nearly unpuckered mean plane. These results justify considering the solid-state structures of α-, β- and γ-CD hydrates, crystallizing with 8–14 water molecules, as relevant "frozen molecular images" of their solution conformations. The solid-state data were used to compute the contact surfaces, cavity dimensions, and molecular lipophilicity patterns (MLPs) of **1**–**3**. The MLPs, presented in color-coded form, provide a lucid picture of how these cyclodextrins are balanced with respect to their hydrophilic (blue) and hydrophobic (yellow) areas: the larger opening of the cone-shaped macrocycles carrying the 2-OH and 3-OH groups is intensely hydrophilic; the opposite, narrower opening, ringed by the CH_2OH groups, is considerably less hydrophilic, and is partially permeated by hydrophobic areas, whereas the bulk of the intensely hydrophobic regions is concentrated on the inner region of the cavities. Thus, the complexation of suitable guest molecules by α-, β-, and γ-cyclodextrin (**1**–**3**), which is governed by a variety of factors, can be rationalized with respect to the hydrophobic interactions on the basis of their MLP profiles. Application of these molecular modelling techniques to the one solid-state structure available for the nine-glucose unit δ-CD tetradecahydrate (**4**) suggests a less pronounced separation of hydrophilic and hydrophobic surface regions, obviously due to a bowl-shaped torus with irregular tilting of four of the nine glucopyranoses which gives rise to substantial pukkering of the macrocycle.

The naturally-occurring cyclooligosaccharides, starch-derived cyclodextrins (CDs), are a family of torus-shaped macrocycles composed of six, seven, eight, or nine α(1 → 4)-linked D-glucopyranose units. They have traditionally been designated with Greek letters: α-CD (**1**), β-CD (**2**), and γ-CD (**3**) are the three most important ones generated by the action of *Bacillus macerans* amylase on starch[2], whereas the δ-CD (**4**) was obtained by special techniques and only in small amounts[3].

All of these have been characterized by their X-ray structures[3,4] and extensive NMR studies[5], as well as force-field based[6–8] and semi-empirical calculations[9] that have been performed on the three major macrocycles **1**–**3**. Their molecular geometries are characterized by the shape of a truncated cone, wherein the 2-OH and 3-OH hydroxyl groups of the respective glucose units occupy the wider rim of the cone. The primary 6-CH_2OH groups occupy the narrower rim side and, accordingly, render the cyclodextrins hydrophilic and soluble in water[2]. On the other hand, the formation of inclusion complexes with a variety of guest molecules provides overwhelming evidence that the inside of the cavity is hydrophobic conceivable due to being walled in by the 3-H and 4-H and by the ether-like intersaccharidic 1-oxygens. In solution, therefore, these cavities provide a hydrophobic space in a hydrophilic surrounding.

The inclusion of neutral molecules into the cyclodextrin cavity involves a variety of different binding interactions, from which the hydrophobic effect[10] is difficult to extract (even if one has agreed on the exact definition of the term). These difficulties notwithstanding, hydrophobic interactions play a dominant role in guest complexations by cyclodextrins – another obvious requirement being that the guest must fit into the cavity even if it is only partially included; thus, an assessment of the hydrophobic features of

[◇] Part 8: Ref.[1].

  0947–3440/96/0101–0027 S 10.00+.25/0

the native cyclodextrins **1**–**4** appeared desirable. Modern molecular modelling techniques[11,12,13] allow the localization of hydrophilic and hydrophobic regions, at least qualitatively, by projection of the computer-generated molecular lipophilicity patterns (MLPs)[12a] onto the contact surfaces. Continuing exploratory studies on the hydrophobic topographies of γ-cyclodextrin (**3**)[14], small ring cyclodextrin analogs[15], several non-glucose cyclooligosaccharides[16], as well as sucrose and a variety of sweeteners[17], we report here a systematic and comparative reappraisal of the hydrophobic and hydrophilic characteristics of cyclodextrins **1**–**4**, based on conformations obtained from a statistical analysis of their solid-state structures[18].

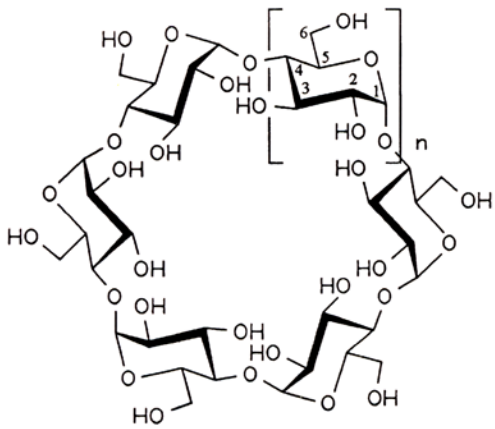

Starch-derived Cyclodextrins

α-CD	**1**	*cyclo*[D-Glc*p* α(1→4)]$_6$
β-CD	**2**	*cyclo*[D-Glc*p* α(1→4)]$_7$
γ-CD	**3**	*cyclo*[D-Glc*p* α(1→4)]$_8$
δ-CD	**4**	*cyclo*[D-Glc*p* α(1→4)]$_9$

Figure 1. Cyclodextrin geometry descriptors: the intersaccharidic bond angle φ is defined by the atoms $C_1-O_1-C_{4'}$, the torsion angles which describe the conformations about the glycosidic linkages are denoted as $\Phi(O_5-C_1-O_1-C_{4'})$ and $\Psi(C_1-O_1-C_{4'}-C_{3'})$. The endocyclic ring torsions around C-4 are designated as $\Theta_1(C_2-C_3-C_4-C_5)$ and $\Theta_2(C_3-C_4-C_5-O_5)$, the exocyclic torsion angle $\omega(O_5-C_5-C_6-O_6)$ describes the orientation of the primary 6-OH relative to the pyranoid ring, whereby the three staggered conformations are referred to as *gauche-gauche* (*gg*, $\omega \approx -60°$), *gauche-trans* (*gt*, $\omega \approx +60°$), and *trans-gauche* (*tg*, $\omega \approx \pm 180°$). The tilt angle τ denotes the inclination of the pyranose rings toward the macrocyclic ring perimeter, i.e. the angle between the cyclodextrin mean plane of all intersaccharidic (i.e. anomeric) oxygen atoms versus the least-squares best-fit mean plane through the six pyranoid ring atoms ($C_1-C_2-C_3-C_4-C_5-O_5$, center plot; hydrogen atoms are omitted for clarity); the normal vector *g* of the latter plane always points to the outside of the macrocycle. Absolute values of $|\tau| > 90°$ indicate the 6-CH_2OH side to be turned towards the central cavity; a positive sign of τ indicates the upper face (clockwise view on C_1-C_5 and O_5) of the sugar moieties pointing towards the outside of the macrocyclic ring. The atomic distances between the anomeric 1-O oxygens diagonally across the macrocyclic ring are denoted $d_{O\text{-}1/O\text{-}1'}$ (lower entry)

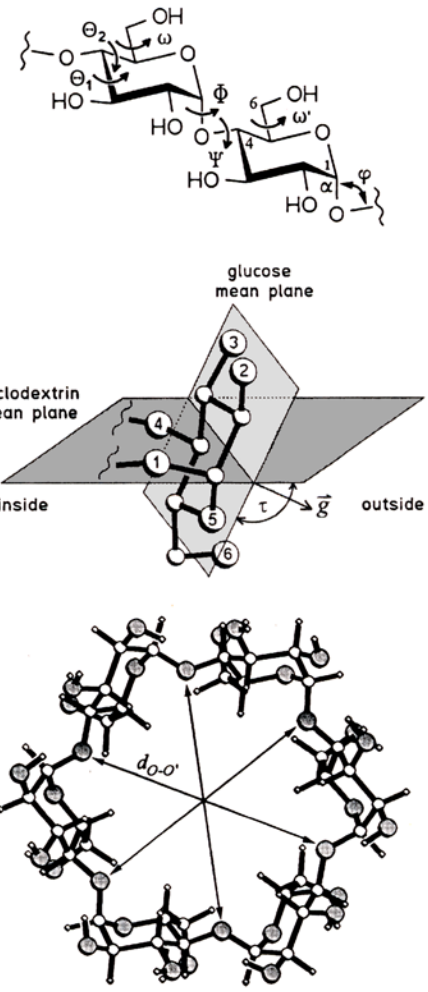

Molecular Geometries of Cyclodextrins 1–4

Statistical analysis of the solid-state geometries of all α-, β-, and γ-cyclodextrin structures contained in the Cambridge Crystallographic data file (CCDF)[19], comprising the hydrates of **1**–**3** as well as their inclusion complexes (98 structures altogether), was performed to obtain their mean molecular geometry parameters as defined in Figure 1. In the case of δ-CD (**4**), the parameters were extracted from a molecular geometry reproduced from a plot of the X-ray structure[20]. The relevant mean structural parameters including their corresponding fluctuations obtained for **1**–**4** are listed in Table 1. All solid-state structures of *per*-2,3,6-*O*- and *per*-2,6-*O*-substituted cyclodextrin analogs (altogether 24 structures of α- and β-cyclodextrins) have been excluded from the analysis procedure, since extensive *O*-substitution can substantially effect the conformational properties of the macrocyclic backbone[4].

Global Molecular Shape. The structure of the cyclodextrins **1**–**4** is determined by the α(1→4)-interglucosidic linkages resulting in essentially unstrained, torus-shaped macrocycles with the primary 6-CH_2OH groups located on one side of the molecule. The opposite, wider aperture is made up of the secondary 2-OH and 3-OH hydroxyl groups. The intersaccharidic bond angle $\varphi(C_1-O_1-C_{4'})$ as well as the glycosidic torsion angles Φ and Ψ are within normal ranges of α(1→4)-type linkages for glucose units (cf. Table 1). A clear illustration of the inclination of the glucose units with respect to the macrocycle is provided by

Table 1. Cyclodextrin mean molecular parameters obtained from statistical crystal structure analysis for α-, β-, γ-, and δ-cyclodextrin geometries[16] (root-mean-square (RMS) deviations in parenthesis)

Cyclodextrin	structures[a] N_1 / N_2	pyranoid ring torsion angles[b] $\langle\Theta_1\rangle$	$\langle\Theta_2\rangle$	pyranose Cremer-Pople parameters $\langle Q\rangle$	$\langle\theta\rangle$	$\langle\phi\rangle$[c]	glucose conformation
α-CD (**1**)	42 / 51	52.3(4.9)	-52.9(6.3)	0.574(0.034)	5.5(4.7)	118.7	$^4C_1$
β-CD (**2**)	48 / 59	55.7(4.3)	-55.9(4.5)	0.579(0.038)	5.0(2.9)	173.5	$^4C_1$
γ-CD (**3**)	8 / 22	62.0(5.9)	-62.3(5.7)	0.613(0.053)	8.5(4.1)	231.2	$^4C_1$
γ-CD (**4**)	1 / 1[d]	53.3	-57.5	0.566	3.6	323.6	$^4C_1$

Cyclodextrin	intersaccharidic torsion angles[b] $\langle\Phi\rangle$	$\langle\Psi\rangle$	angle[e] $\langle\varphi\rangle$	tilt[f] $\langle\tau\rangle$	atomic distances [Å] $\langle O_1\text{-}O_{1n'}\rangle$[g]	$\langle O_2\text{-}O_{3'}\rangle$	$\langle C_6\text{-}C_{6'}\rangle$
α-CD (**1**)	108.1(6.3)	130.3(7.6)	118.4(2.0)	101.4(5.9)	8.50(0.22)	3.05(0.55)	4.47(0.21)
β-CD (**2**)	111.9(6.8)	127.6(8.0)	117.7(2.6)	99.5(7.1)	9.83(0.24)	2.92(0.27)	4.64(0.34)
γ-CD (**3**)	109.9(3.2)	129.6(3.5)	115.0(3.1)	104.5(2.4)	11.76(0.07)	2.84(0.06)	4.39(0.30)
γ-CD (**4**)	112. (16.)	122. (19.)	118.9(8.1)	105. (24.)	12.46(1.23)	3.01(0.19)	4.66(0.50)

[a] A total of N_1 different solid-state structures with N_2 crystallographically independent cyclodextrin molecules were analyzed. – [b] Φ: $O_5-C_1-O_1-C_{4'}$, Ψ: $C_1-O_1-C_{4'}-C_{3'}$, Θ_1: $C_2-C_3-C_4-C_5$, Θ_2: $C_3-C_4-C_5-O_5$. – [c] for $\theta \rightarrow 0°$, the puckering angle φ and the corresponding RMS deviations become meaningless, since $^4C_1$-conformations are identical to $^2C_5$ and $^0C_3$. – [d] due to the mode of generation of the single δ-CD structure (see text) the RMS fluctuations of some molecular parameters are irrelevant. – [e] φ: $C_1-O_1-C_{4'}$. – [f] angle between best-fit mean plane of the macro ring (defined by all O_1 atoms) and each glucose-mean plane (atoms C_1 to C_5 and O_5). – [g] $O_1-O_{1n'}$ distances (in Å) diagonally across the cyclodextrin ring.

the tilt angles τ as defined in Figure 1. Their mean values around 100–105° (cf. Table 1) correspond to a canting of the 6-CH_2OH groups towards the center cavity ($\tau > 90°$). Accordingly, these groups form the smaller opening of the cyclodextrin ring. On the opposite molecular side, the 2-OH/3-OH section points away from the molecular axis, molding the wider torus rim.

The width of the probability distributions of the tilt angle (Figure 2) and the corresponding root-mean-square (RMS) fluctuations (Table 1) indicate a certain degree of flexibility for α-CD (**1**) and even more so for β-CD (**2**). In the case of γ-CD (**3**) with its eight glucose units, the comparatively narrow τ-distribution range (≈105 ± 5° in Figure 2) suggests that it seems to prefer symmetrical overall conformations with somewhat limited intersaccharidic flexibility. The opposite holds true for the δ-CD (**4**): the widespread distribution of different glucose inclinations in the solid-state structure indicates that steric strains introduced by increasing the CD ring size can be compensated by asymmetric deformation of the entire macrocycle. Thereby, the extended conformational space accessible to the nine glucose moieties by rotation around the intersaccharidic linkages results in an increased overall molecular flexibility.

An analogous trend is observed for the atomic distances between the intersaccharidic linkage oxygens lying diagonally across the macrocyclic ring (Figure 3): the comparatively wide distribution of mean diameters found for α-CD (≈8.5 ± 0.5 Å) and β-CD (≈9.8 ± 0.6 Å) are contrasted by a distinctly narrower range for the γ-CD (≈11.8 ± 0.1 Å). This again illustrates the pronounced tendency of the γ-CD to form almost perfectly symmetrical structures. The δ-CD (**4**), however, is highly flexible and thus adaptable to various distortions of the macrocycle – a statement of limited scope as it is based on only one example.

Figure 2. Probability distribution of glucose tilt angles τ observed in the crystal structures of α-, β-, γ-, and δ-cyclodextrins

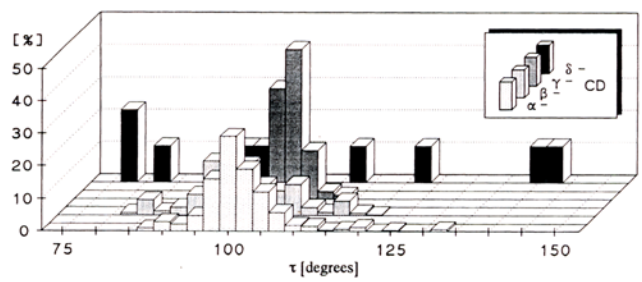

Figure 3. Percentage distribution of the distances between intersaccharidic oxygens (O-1 ↔ O-1′) diagonally across the macrocyclic ring (in Å) in relation to the CD ring size as retrieved from crystal structural data

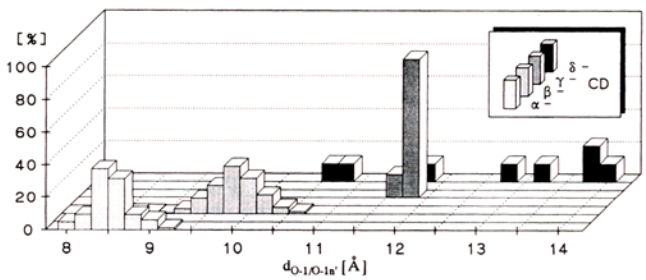

Pyranoid Ring Conformation. As is clearly evident from the pyranoid torsion angles – only two are listed in Table 1, namely Θ_1 ($C_2-C_3-C_4-C_5$) and Θ_2 ($C_3-C_4-C_5-O_5$) describing the conformational relationships around C-4 of the glucose residues – the glucopyranose units in each of the four cyclodextrins invariably adopt the standard $^4C_1$ conformation with surprisingly small deviation from the ideal, that is, entirely undistorted values. By considering the heavy atoms C-1 to C-6 and O-1 to O-5 (but not O-6), the least-squares fitting of all glucose units via rigid body translation and rotation[21] showed root-mean-square (RMS) fluctuations of the atomic positions of only approximately 0.07 Å. In addition, the Cremer-Pople ring-puckering parameters[22] for the pyranoid segments, in particular the puckering angle θ of approximately 0.0 to 10.0°, are consistent with uniform $^4C_1$ geometries for any of the glucose moieties.

Actually, there seems to be only one example, namely an inclusion compound of the per-*O*-methylated β-cyclodextrin, in which one of the seven glucose units adopts a $^0S_2$ skew (twist boat) conformation in the solid-state (recalculated parameters $Q = 0.722$ Å, $\theta = 86.7°$, and $\phi = 323.6°$) that is caused by a guest-induced conformational transition to relieve the steric hindrance of the 2-OMe and 3-OMe groups[23]. Thus, deviations from the $^4C_1$ geometry of the glucose moieties either require steric hindrance engendered by *O*-substitution in the sugar portion and a guest molecule, or alternately, a decrease in the number of glucose units to five, four, or three. The hypothetical *cyclo*-α(1→4)-glucotetraoside and its trioside analog, for example, exhibit envelope (E_1) conformations in their pyranoid rings[15].

2-O···O-3′-Interresidue Distances. Characteristic for the cyclodextrins are the comparatively short distances between the glucosyl-2-oxygen (2-O) and the 3-oxygen of the next glucosyl moiety (3′-O). As illustrated in Figure 4, the mean 2-O···O-3′ distances become smaller on increasing the macrocyclic ring size from six to seven and eight glucose units, that is, α-CD > β-CD > γ-CD. The close contact between these two oxygen atoms undoubtedly favors 2-O···HO-3′ hydrogen bonding. This type of intramolecular interaction is not limited to only the solid-state structures of CD's[4,24], but it also prevails in solution as was established by IR experiments[25]. Thereby, the decreasing distances account for the larger conformational flexibility of α-CD in relation to its larger homologs β- and γ-CD[2c]. This favorable hydrogen bonding interaction not only decreases the chemical reactivity of the 3-OH group dramatically[25], it is also responsible for the considerably enhanced reactivity of the 2-OH groups – in particular when compared to the primary 6-OH – in the course of the sodium hydride-induced alkylation of the CDs[26], for example. The 2-alkoxide anions generated under these conditions are effectively stabilized by intramolecular hydrogen bonding between adjacent O-2 and O-3′ oxygen atoms[27], leading to a concentration of the main charge density at O-2. Consequently, the ensuing trapping reaction of the anions with alkylating agents is characterized by a high regioselectivity for the glucose-2-OH[26], similar to the selectivities found for the alkylation of sucrose[1,28].

Figure 4. Mean O–O-distances between the 2-oxygen of one glucose moiety and the 3-oxygen of the next

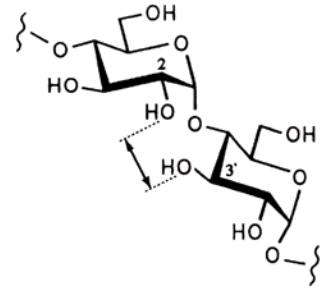

2-O ··· O-3' distances	
α-CD	3.06 Å
β-CD	2.92 Å
γ-CD	2.84 Å
(δ-CD	3.01 Å)

Conformational Arrangements of the 6-CH_2OH Groups. The orientation of the 6-hydroxymethyl group in relation to the pyranoid ring in hexoses is defined by two torsion angles $O_5-C_5-C_6-O_6$ (≡ ω) and $C_4-C_5-C_6-O_6$. In principle, the ω angle can have any value in the −180° to +180° range, but generally the conformations to be considered are the three staggered ones, referred to as *gauche-gauche* (*gg*), *gauche-trans* (*gt*), and *trans-gauche* (*tg*) forms (cf. Figure 5). The first letter denotes the orientation of O-6 towards the pyranoid ring oxygen, whereas the last letter describes the relationship relative to C-4. Generally, the rotamer population of the hydroxymethyl groups in relation to the pyranoid rings is such that, of the three staggered conformations, the *tg* form is the least favored due to 1,3-diaxial-like repulsions between O-4 and O-6[24,29,30].

Figure 5. The three staggered conformations of the 6-CH_2OH in glucose, denoted by the position of the 6-O relative to the atoms at the C_5-C_6 bond

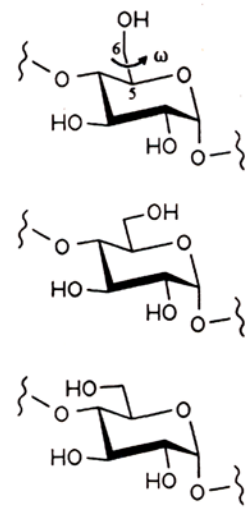

From the altogether 99 cyclodextrin solid-state structures (inclusion complexes included) that have been screened for their 6-CH_2OH rotameric forms, a clear picture evolves: the occurrence of the *gg* form is favored over the *gt* rotamer by an approximately 3.5:1 ratio (Figure 6). Accordingly, the form in which the 6-OH points towards the outside of the

macrocyclic ring is the preferred one. Most notably, not a single case of a *tg* conformation was encountered.

Macrocyclic Ring Flexibility. The multitude of the α-CD, β-CD, and γ-CD structures that have been comparatively analyzed here display a considerable degree of flexibility in the macrocyclic rings that represent truncated-cone structures which are by no means rigid. This also evolves from various force-field-based and semi-empirical computational studies[7–9], from extensive molecular dynamics simulations[6], and from a detailed high-temperature annealing (HTA) investigation of α-CD[15].

Figure 6. Probability distribution of the conformations of the hydroxymethyl groups (ω torsion angle, top) derived from α-, β-, γ-, and δ-cyclodextrin solid-state geometries (altogether 133 crystallographically independent molecules in 99 different structures). They clearly reveal a 3.5:1 distribution of *gg* and *gt* rotamers (ω ≈ −60° and +60°, respectively), and not a single case of a *tg* conformation. The uniform conformation of the linkages between the monosaccharide units within all CD-structures is born out by the scatter plot of the intersaccharidic Φ/Ψ torsion angles (bottom), in which the respective mean values and root-mean-square (RMS) deviations of Φ and Ψ are marked by solid and dotted lines

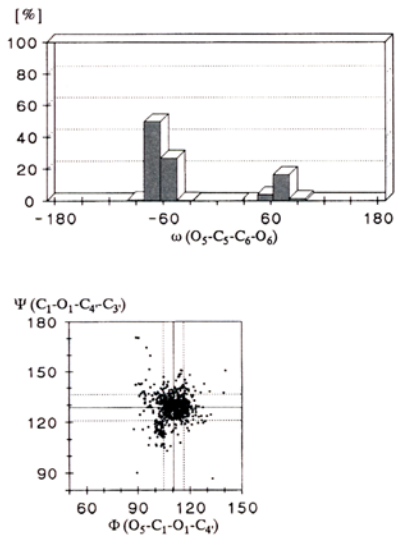

On the other hand, the overall puckering of the macrocyclic rings is generally small. This is most clearly illustrated by the 99 X-ray structures analyzed (comprising a total 133 independent geometries) in which the intersaccharidic ring oxygens, all pointing toward the interior of the central cavity, essentially lie in one plane. The average deviations from this plane are in the ±0.1 Å range only, that is, ±0.07 Å for the six anomeric oxygens in α-CD (**1**), ±0.10 Å for β-CD (**2**), and most notably, only ±0.02 Å for the eight intersaccharidic oxygens in the γ-CD (**3**)[31]. The δ-CD (**4**) was not included in these considerations as there is only one X-ray structure available[3] in which the macrocycle is significantly distorted (average displacements of all O-1 atoms are as large as ±0.7 Å).

Solid-State Structures of Cyclodextrin Hydrates as Models for "Empty" Solution Conformations

As all the cyclodextrins were crystallized from aqueous solutions, they contain various amounts (6–13%) of water. In the case of α-CD (**1**), depending on the conditions applied for crystal growth, three different polymorphic forms have been characterized: α-CD · 6 H_2O, form I[32] and form II[33], as well as an α-CD · 7.57 H_2O, form III[34]. The latter species of α-CD is nearly symmetrical with 2.57 water molecules being statistically distributed over four alternative positions inside the cavity. The other two forms exhibit nearly identical, conically distorted shapes for the macrocycle, whereby one glucose unit is strongly tilted towards the center of the molecule (τ = 132° as compared to an average of 98° for the others). Thus the cavity becomes oblique – this can be described as partially "symmetry collapsed" – due to the optimization of the hydrogen bonding interactions between the cyclodextrin and the water of crystallization to reduce "empty volume". However, α-CD is able to expand to a more symmetrical macrocyclic ring on formation of inclusion complexes[32] or on dissolution in water. A comparative molecular dynamics (MD) simulation of α-CD in the crystalline state and in aqueous solution indicated that the inclination of the glucose residue, observed in the crystalline forms I and II, disappears upon dissolution, resulting in a conformation closely resembling form III, while the asymmetric overall shape of the molecule seems to be retained to some extent[6]. These results receive further support from a ^{13}C-(CP-MAS)-NMR study indicating that the "partially symmetry-collapsed" solid-state geometry is released in water[35].

The two β-cyclodextrins hydrates, that is, β-CD · 12 H_2O[36,37] and β-CD · 11 H_2O[37,38], show nearly symmetrically opened, round shapes of their tori, that are not dramatically changed upon formation of inclusion complexes. Their main structural differences lie in the distribution of disordered water molecules within the host cavity, whereby the 6–6.5 water molecules are statistically distributed over eight crystallographic positions. Neutron diffraction analysis at room temperature and at 120 K revealed a flip-flop type hydrogen bonding pattern with a high thermal flexibility even in the solid-state[38]. These characteristics of β-cyclodextrin were corroborated by MD simulations of hydrated crystalline β-CD at different temperatures[6c,d], which revealed no significant conformational changes between the crystalline state and the solution conformation[39]. Also, a solid-state ^{13}C-NMR investigation of the slow dehydration of β-CD from 12 to 10.5 H_2O molecules indicated no loss of crystal order, nor any phase transition[39]. This is in contrast to α-CD, where partial dehydration of the crystals is accompanied by major structural changes.

For the non-complexed γ-CD, three solid-state structural analyses have been put forth containing varying amounts of co-crystallized water (γ-CD · 17 H_2O[40], ≈ 14 H_2O[41], and 15.7 H_2O[42]), of which 5.3–8.8 water molecules are randomly distributed in the cavity over approximately twice as many different positions. The former, low-temperature structure (120 K) shows significant distortions from an ideal octagonal molecular symmetry[40]. These distortions are related to the disordering of one of the glucose residues; yet the other two geometries are almost perfectly rounded

Figure 7. Ball-and-stick model representations of the solid-state structure based molecular geometries and dotted contact surfaces of the cyclodextrins **1**–**4** containing six, seven, eight, and nine α(1→4)-linked glucose units, respectively. Structures are shown perpendicular to the mean ring plane of the macrocycles and are viewed through the large opening of the conically shaped molecules, i.e. the 2-OH/3-OH side of the pyranoid rings points towards the viewer, and the primary 6-CH_2OH groups away from him, towards the back; oxygen atoms are shaded

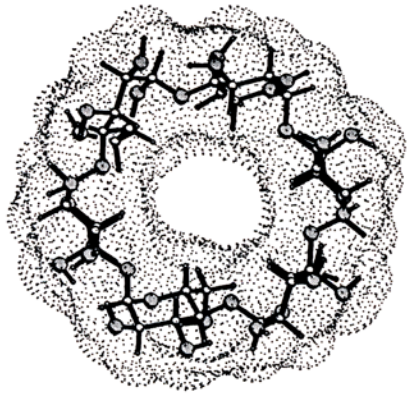

α-Cyclodextrin
cyclo[D-Glc*p* α(1→4)]$_6$

β-Cyclodextrin
cyclo[D-Glc*p* α(1→4)]$_7$

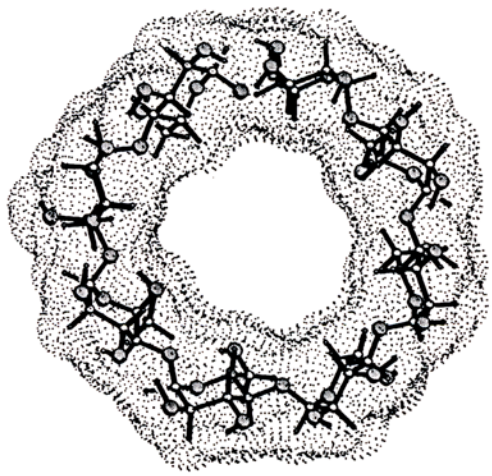

γ-Cyclodextrin
cyclo[D-Glc*p* α(1→4)]$_8$

δ-Cyclodextrin
cyclo[D-Glc*p* α(1→4)]$_9$

with only slight annular distortions[41,42]. Thus, they represent by far the most symmetrical structures encountered in the entire series of CD hydrates. This is also born out by a recent force field-based study which noted the remarkably high agreement of the γ-CD · 14 H_2O structure[41] with the fully optimized MM2-geometry conformation[43].

For the nine-glucose unit δ-CD (**4**) only one X-ray structure (for δ-CD · 13.75 H_2O[3]) is available, and any conclusion drawn therefrom is limited in scope. The data on **4**, however, suffice to indicate a high flexibility, as the torus adopts a bowl-shape rather than a planar structure: four out of the nine glucose units are canted to a large extent with their primary 6-OH groups towards the center cavity, while the others line up almost perpendicular to the macrocyclic ring or are even inclined towards the opposite direction. The 2-OH/3-OH aperture is opened much wider than the opposite 6-CH_2OH side, and the range for the tilt angle ($\tau = 77-141°$, cf. Figure 2) is unusually large.

To summarize, the general picture that emerges is one in which the heavily hydrated solid-state conformations of the four cyclodextrins – as well as most of their inclusion complexes – can be regarded as *relevant snaphshots of their overall shape in aqueous solution*, in a sense representing "frozen molecular images". Accordingly, we have chosen the most symmetrical and unstrained CD hydrate structures – α-CD · 7.57 H_2O (form III)[34], β-CD · 11 H_2O[38], γ-CD · 14 H_2O[41], and δ-CD · 13.75 H_2O[3], all X-ray structures except of β-CD, for which the neutron diffraction geometry was used – as reliable models for CD structures in (aqueous) solution. They also represent the starting points for

Figure 8. Cross section plots of a plane perpendicular to the macrocycle mean plane with the contact surfaces of the cyclodextrins **1**–**4**. Contours were obtained for successive 10° rotation steps around the geometrical center M and superimposed. In each case, the widely opened torus rim of the secondary 2-OH/3-OH groups is on top, and the narrow aperture made up by the primary 6-OH groups on the bottom; approximate molecular dimensions are included

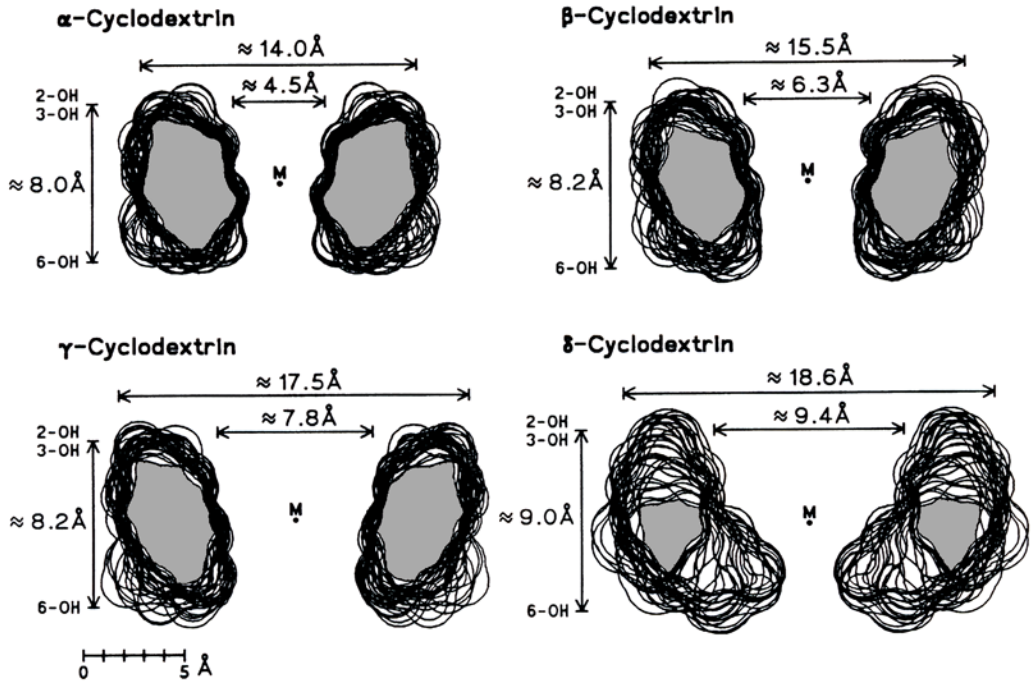

Table 2. Molecular dimensions and cavity characteristics of cyclodextrins **1**–**4**

Cyclodextrin	Torus Ø [Å] outer	inner	Torus height	Surface area [Å²] total	cavity	Molecular volume [Å³] total	cavity	exp.[a]
α-CD (**1**)	14.2	5.2	8.0	720	85	975	100	1010
β-CD (**2**)	15.7	6.6	8.0	845	105	1140	160	1168
γ-CD (**3**)	17.3	8.4	8.0	960	140	1305	250	1330
δ-CD (**4**)	≈18.6	≈9.4	≈8.0	1075	–[b]	1450	–[b]	–

[a] Apparent molar volume $^{\Phi}V$ for dilute aqueous solutions[47]. – [b] Deformation of the macrocycle does not allow a clear-cut definition of the cavity dimensions.

probing into the hydrophobic topographies of the cyclodextrins by molecular modelling.

Cyclodextrin Contact Surfaces and Cavity Dimensions

In our study on small ring cyclodextrins[15] we have noted the relevance of molecular contact (Connolly-type) surfaces[44] as estimations of solvent-accessible molecular regions[45]. Thus, the molecular surfaces of the four cyclodextrins were generated with the MOLCAD program[11] starting from their respective solid-state structures of their hydrates (cf. above). In Figure 7, the molecular geometries are shown with the corresponding surfaces being superimposed in dotted form. For better visualization of the extension of these surfaces and the cavity proportions, cross cuts through the contact surfaces were calculated and the respective contour lines originating from successive 10° rotation around the geometrical center M were superimposed (Figure 8).

The cavity interior comprises approximately 10–15% of the total cyclodextrin surface area (Table 2, ≈120 Å²/glucose unit)[46]; it increases from approximately 85 Å² in α-CD, to 105 Å² (β-CD) and 140 Å² in the γ-CD (Table 2). The spatial volume enclosed by the contact surfaces closely corresponds to the apparent molar volume $^{\Phi}V$ demanded by these compounds in aqueous solution. The agreement between the values calculated for the cyclodextrins **1**–**3** (Table 2, ≈160–165 Å³/glucose unit) and the volumes $^{\Phi}V$ obtained from density measurements in aqueous solution[47] indicates that the central hole is occupied by water molecules; otherwise, much larger apparent volumes would be observed.

Correspondingly, on the basis of the apparent molar volume of water ($^{\Phi}V_{H_2O}$ ≈ 18 cm³/mol ≈ 30 Å³/molecule), it can be concluded that 2–3 water molecules fit into the α-CD cavity, while β-CD is able to accommodate approximately five, and γ-CD even 8–9 water molecules. The obviously good agreement with the solid-state structural data for the respective CD hydrates (vide supra) indicates the usefulness of this type of surface for evaluating the steric features of the CDs.

The irregular shaped intersection contours computed for the δ-CD are directly related to its significantly puckered macrocyclic conformation. The same holds true for the apparently increased height of the δ-CD tours of ≈9.0 Å, while for the other CD classes usually 8.1 ± 0.1 Å are measured, however, when applying a correction to account for the large CD puckering, the effective height of the δ-CD falls into the same range.

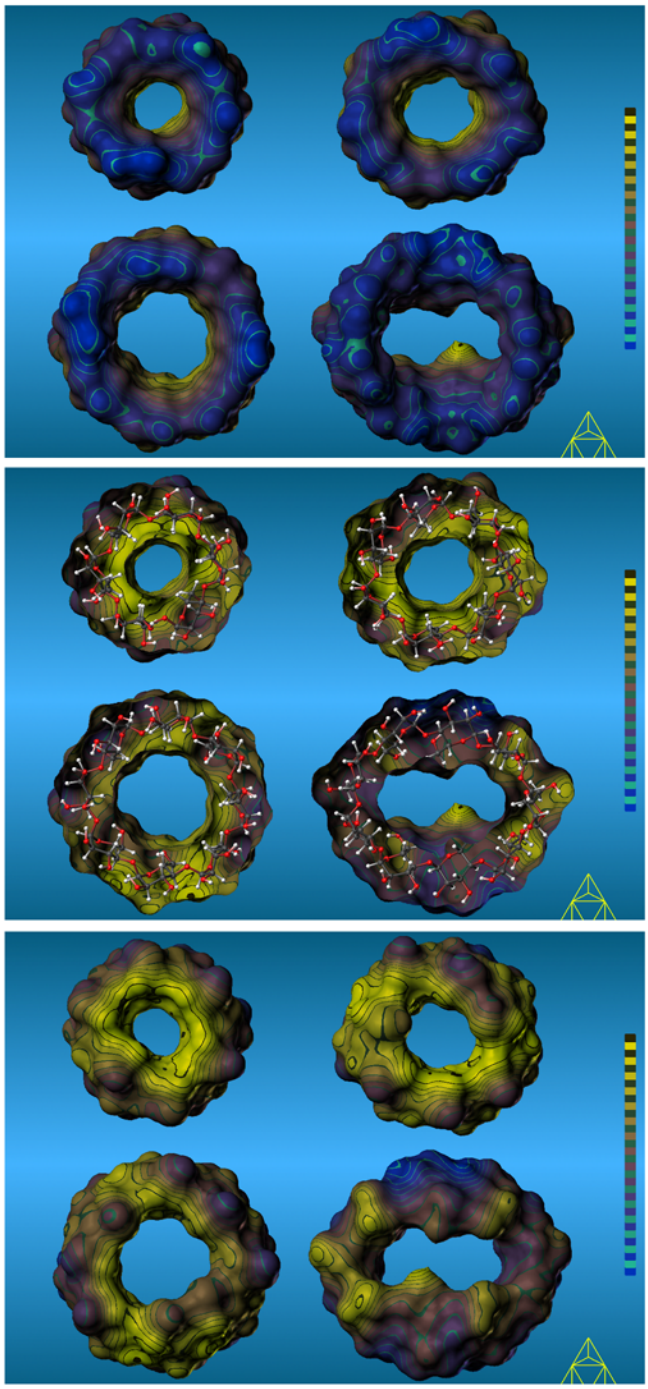

Figure 9. MOLCAD-program generated molecular lipophilicity patterns (MLP) projected onto the contact surfaces of α-CD (**1**, upper left), β-CD (**2**, upper right), γ-CD (**3**, lower left), and δ-CD (**4**, lower right). For visualization a two-color-code graded into 32 shades is used. The color-coding was adapted to the range of relative hydrophobicity calculated for each molecule by using 16 colors ranging from dark blue (most hydrophilic surface areas) over light blue to full yellow (most hydrophobic regions) for mapping the computed values onto the surface. The remaining 16 color shades (light blue to brown) were used to indicate iso-contour lines in between former color scale, allowing a more quantitative assessment of relative hydrophobicity on different surface regions. The top picture views through the larger openings of the conically shaped molecules, thus exposing the intensively hydrophilic (blue) 2-OH/3-OH side. In the middle, the hydrophilic front half of the surfaces has been removed providing an inside view onto the hydrophobic (yellow) back; in addition, a ball-and-stick model was inserted to illustrate the molecular orientation (mode of viewing analog to Figure 7). The bottom representation depicts the "back" of the cyclodextrins (i.e. the smaller opening with the 6-CH_2OH groups facing the viewer; models were rotated by 180° around a vertical axis), clearly exposing the hydrophobic (yellow) surface areas, that in the case of **1**, **2**, and **3** extend well into the cavity

The torsi diameters and cavity dimensions displayed in Figure 8 represent a first approximate criterion to judge the steric limitations required for the formation of inclusion complexes. Given the conformational flexibility of the cyclodextrins to adapt to different shapes and sizes of guest molecules, it becomes obvious that not only small molecules such as MeOH[48], DMF[49], and DMSO[50] but also various mono- or di-substituted benzene derivatives[51] and inorganic metal complexes[52] fit well into the α-CD cavity. β-CD is able to include aromatic compounds carrying sterically more demanding substituents like 4-*tert*-butylbenzyl alcohol[53], 4-*tert*-butyl-benzoic acid[54], and 4-*tert*-butyltoluene[55], for example, or even spherically shaped guests like hexamethylenetetramine[56], adamantane[57], or substituted its derivatives[58]. γ-CD can accommodate almost perfectly rounded 12-crown-4 ether complexes[59,60], or even such crowded compounds as 1,2,3-tri-*tert*-butylnaphthalene[61], and C_{60}, bi-capped by two γ-CDs[62]. For δ-CD, no inclusion complexes have been described, but on the basis of its molecular dimensions it was surmised[3], that a naphthalene molecule would be "included loosely or rather freely, and an anthracene seems to fit well".

Molecular Lipophilicity Patterns of Cyclodextrins 1–4

Aside from the imperative fulfilment of steric requirements, the hydrophobic effect[10] represents the most important factor in governing guest-host interactions in the cyclodextrin series[2]. The concomitant release of complexed water from the cyclodextrin cavity as well as from the hydrophobic hydration sphere[10] of the guest, and its incorporation into the bulk aqueous phase, must be considered as the main entropic factor favoring complex formation. However, this favorable contribution to entropy is usually counteracted by the loss of degrees of freedom from combining two independent molecules into one complex and, hence, the complexation by cyclodextrins is enthalpy-driven in most cases[63].

The color-coded visualization of molecular lipophilicity patterns (MLP)[12a] projected onto molecular contact surfaces by using the MOLCAD molecular modelling program[11,12b] is especially suited for the assessment of hydrophobic interactions[13]. The MLPs for the four cyclooligosaccharides **1**–**4** were projected onto the corresponding molecular contact surfaces, and are depicted in Figures 9 and 10 in a two-color-code graded into 32 shades, ranging from dark blue for the most hydrophilic areas to yellow for the most hydrophobic regions.

The lipophilicity patterns of the α-, β- and γ-cyclodextrins reveal the 2-OH/3-OH side of the macrocycles, that is, the wider torus rim, to be distinctly hydrophilic as evidenced by the clearly defined blue areas (Figure 9, top).

Figure 10. Side view MLPs, in closed and bisected form each, of the four α(1→4)-cyclodextrins **1**–**4** with six (**1**, α-CD, upper left), seven (**2**, β-CD, upper right), eight (**3**, γ-CD, lower left), and nine (**4**, δ-CD, lower right) glucose units, respectively; color coding according to Figure 9. Their orientation is such that the 2-OH/3-OH side is always aligned upward (larger opening of the torus) and the 6-CH_2OH points downward (smaller aperture, molecular orientation cf. Figure 8). The similarities in the distribution of hydrophilic (blue) and hydrophobic surface areas – most notably on the inside regions of the cavities of **1**, **2**, and **3** – are clearly apparent

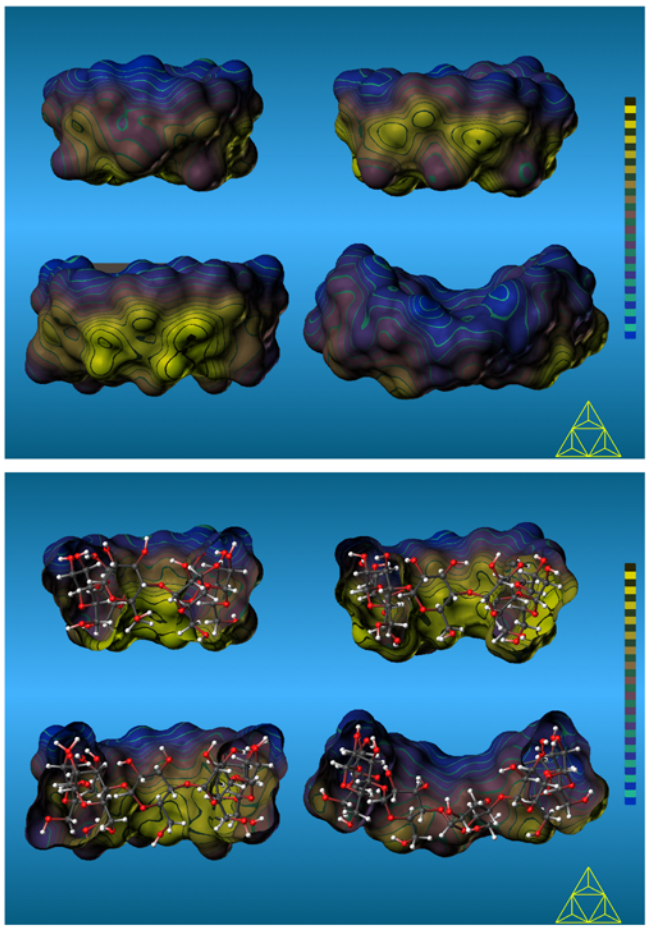

This is contrasted with the intensely hydrophobic (yellow) surface regions (Figure 9, center and bottom) on the opposite side – the narrower opening made up by the 6-CH_2OH groups – which is obviously caused by the close spatial arrangement of the 6-CH_2- and the $O_5-C_5-H_5$ fragments of all glucose residues. In the case of the nine-glucose homolog, δ-CD **4**, the separation of hydrophobic and hydrophilic surface areas between the front and back of the molecule becomes less pronounced, obviously a consequence of the considerably larger puckering of the macrocycle and the irregular tilting of the glucose moieties.

Out of the calculated total surface area of ≈120 $Å^2$ per glucose unit (α-CD: 720, β-CD: 845, γ-CD: 960, and δ-CD: 1075 $Å^2$) approximately 10% contribute to the inner surface of the central cavity (α-CD: 85, β-CD: 105, and γ-CD: 140 $Å^2$, for δ-CD an exact value cannot be obtained). Most notably, it is invariably this inner area of the molecular surface which is calculated to be the most hydrophobic in all cases (cf. Figure 10).

Coda[64]

The molecular modellings presented here provide a concise picture of cyclodextrin features – in terms of their geometrical and conformational properties as well as their molecular lipophilicity patterns – as a function of their size. At first, the choice of the CD structures utilized in this study may seem arbitrary. However, their use is supported by computational studies and NMR investigations that vindicate this selection of CD hydrates to represent relevant "frozen molecular images" of their solution states. When all the facts are gathered, they indicate that the molecular lipophilicity patterns reveal rather uniform hydrophobic topographies of all CDs that are nearly independent of their ring size. Variations in the glucose tilt angles are moderate and rotations of the hydroxymethyl groups neither alter the MLP patterns significantly, nor do they change their basic implications; they may thus be considered an "adaptive fine tuning".

The multitude of structures presented here provide further corroborations for the pivotal importance of hydrophobic interactions for the formation of the inclusion complexes, which in combination with polarization effects, dipole-dipole attractions, and Van der Waals interactions are responsible for their remarkable stability. Enthalpic and entropic thermodynamic parameters counteract each other at least partially, and the relative contribution of each of the basic types of interactions to the total free energy of binding undoubtedly varies with the nature of the guest. Thus, no attempts are, or should be, made to propose a single gradation of universal validity on the relevance of the various effects. Experimental studies suffer from the currently prevailing dilemma that all types of interactions are almost inseparably interconnected, and thus, preclude an exact and unequivocal factorization of the Gibbs energy into various energy and entropy terms. Actually, it may well be, that computational strategies, such as the one presented here, provide tools sophisticated enough to study experimentally inaccessible features on a basic molecular level. These strategies thus substantially contribute to a more profound understanding of the causative factors underlying the formation of cyclodextrin inclusion complexes. This process, in a figurative sense, is more appropriately visualized as an induced-fit mechanism[65] encompassing guest-induced conformational changes in the host, rather than as a rigid lock-and-key type[66] steric fit.

It is obvious, to judiciously apply the molecular modelling techniques, used here for "empty" cyclodextrin hydrates, to actual inclusion complexes. These studies are to be described elsewhere[67].

We are most grateful to Prof. Dr. *J. Brickmann*, Institut für Physikalische Chemie of this University, for generously providing us the MOLCAD modelling software package[11] and his sophisticated computational facilities.

Experimental

Molecular Structures: All cyclodextrin geometries were obtained from the Cambridge Crystallographic data base[19]; more recent

structure determinations were included as long as the atomic coordinates had been provided; structures of *per*-2,3,6-*O*- and *per*-2,6-*O*-substituted cyclodextrin derivatives were not considered for statistical analysis. Hydrogen atoms not included in the molecular structures were positioned geometrically with standard bond lengths $r_{C-H} \approx 1.08$ Å and $r_{O-H} \approx 0.90$ Å, taking special care of possible intramolecular hydrogen bonding between neighboring hydroxyl groups. All given molecular parameters discussed within this study had been recalculated from this data set.

Geometry of δ-Cyclodextrin (**4**)[20]: From rigid-body rotation and least-squares fitting[21] of the glucose residues of all α-, β-, and γ-CDs, two mean glucose units (C_6O_6) with orientations of the hydroxymethyl grouping being either *gg* or *gt* were obtained. The atomic coordinates of δ-CD units were generated by rotation of these standard glucose units and least-squares fitting of their projections to each of the glucose moieties in the δ-CD plot in ref.[3]. Subsequent assembly of all reoriented residues by fitting the O_1 atoms together yielded the overall conformation of the macromolecule with mean uncertainties in the coordinates of the O_1 atoms of ≈0.03 Å; hydrogen atoms were placed geometrically as described above.

Molecular Surfaces and Molecular Lipophilicity Patterns: Calculation of the molecular contact surfaces and MLPs was carried out by using the MOLCAD[11] molecular modelling program and texture mapping[12b]. Scaling of the hydrophobicity profiles was performed in arbitrary units and in relative terms for each molecule separately, and no absolute values are displayed (no significant differences are observed by applying absolute overall scaling). Color graphics were photographed from the computer screen of a SILICON-GRAPHICS workstation.

☆ Dedicated to Professor *András Lipták*, Kossuth University, Debrecen, on the occasion of his 60th birthday.

[1] Part 8: F. W. Lichtenthaler, S. Immel, P. Pokinskyj, *Liebigs Ann.* **1995**, 1939–1948.

[2] [2a] F. Cramer, *Einschlußverbindungen*, Springer-Verlag, Berlin/Heidelberg, **1954**. – [2b] W. Saenger, *Angew. Chem.* **1980**, *92*, 343–361; *Angew. Chem. Int. Ed. Engl.* **1980**, *19*, 344–362. – [2c] W. Saenger, *Structural Aspects of Cyclodextrins and their Inclusion Complexes*, in: *Inclusion Compounds* (Eds.: J. L. Atwood, J. E. D. Davies, D. D. MacNicol), Acad. Press, London, **1984**, Vol. 2, pp. 231–259. – [2d] R. J. Clarke, J. H. Coates, S. F. Lincoln, *Adv. Carbohydr. Chem. Biochem.* **1988**, *46*, 205–249. – [2e] D.Duchêne (Ed.), *Cyclodextrins and their Inclusion Complexes*, Edition de la Santé, Paris, **1987**. *New Trends in Cyclodextrins and Derivatives*, Edition de la Santé, Paris, **1991**. – [2f] G. Wenz, *Angew. Chem.* **1994**, *106*, 851–870; *Angew. Chem. Int. Ed. Engl.* **1994**, *33*, 803–822.

[3] T. Fujiwara, N. Tanaka, S. Kobayashi, *Chem. Lett.* **1990**, 739–742.

[4] K. Harata, *Recent Advances in the X-Ray Analysis of Cyclodextrin Complexes*, in: *Inclusion Compounds* (Eds.: J. L. Atwood, J. E. D. Davies, D. D. MacNicol), Oxford Univ. Press, Oxford, Vol. 5, **1991**, pp. 311–344.

[5] Y. Inoue, *Ann. Rep. NMR Spectrosc.* **1993**, *27*, 59–101.

[6] [6a] J. E. H. Koehler, W. Saenger, W. F. van Gunsteren, *Eur. Biophys. J.* **1987**, *15*, 197–210; *J. Mol. Biol.* **1988**, *203*, 241–250. – [6b] J. E. H. Koehler, W. Saenger, W. F. van Gunsteren, *J. Biomol. Struc. Dyn.* **1988**, *6*, 182–198. – [6c] J. E. H. Koehler, W. Saenger, W. F. van Gunsteren, *Eur. Biophys. J.* **1987**, *15*, 211–224; **1988**, *16*, 153–168. – [6d] A. E. Mark, S. P. van Helden, P. E. Smith, L. H. M. Janssen, W. F. van Gunsteren, *J. Am. Chem. Soc.* **1994**, *116*, 6293–6302.

[7] H. Dodziuk and K. Nowinski, *J. Mol. Struc. (THEOCHEM)* **1994**, *110*, 61–68.

[8] K. B. Lipkowitz, *J. Org. Chem.* **1991**, *97*, 6357–6367.

[9] I. Bakó, L. Jicsinszky, *J. Inclusion Phenom. Mol. Recogn. Chem.* **1994**, *18*, 275–289.

[10] W. Blokzijl, J. B. F. N. Engberts, *Angew. Chem.* **1993**, *105*, 1610–1624; *Angew. Chem. Int. Ed. Engl.* **1993**, *32*, 1545–1579.

[11] [11a] J. Brickmann, *MOLCAD – MOLecular Computer Aided Design*, Technische Hochschule Darmstadt, **1992**. The major part of the MOLCAD program is included in the SYBYL package of TRIPOS Associates, St. Louis, USA. – [11b] J. Brickmann, *J. Chim. Phys.* **1992**, *89*, 1709–1721. – [11c] M. Waldherr-Teschner, T. Goetze, W. Heiden, M. Knoblauch, H. Vollhardt, J. Brickmann, in: *Advances in Scientific Visualization* (Eds.: F. H. Post, A. J. S. Hin), Springer Verlag, Heidelberg, **1992**, pp. 58–67. – [11d] J. Brickmann, T. Goetze, W. Heiden, G. Moeckel, S. Reiling, H. Vollhardt, C.-D. Zachmann, *Interactive Visualization of Molecular Scenarios with MOLCAD/SYBYL*, in: *Insight and Innovation in Data Visualization* (Ed.: J. E. Bowie), Manning Publications Co., Greenwich, **1994**, pp. 83–97.

[12] [12a] W. Heiden, G. Moeckel, J. Brickmann, *J. Comput.-Aided Mol. Des.* **1993**, *7*, 503–514. – [12b] M. Teschner, C. Henn, H. Vollhardt, S. Reiling, J. Brickmann, *J. Mol. Graphics* **1994**, *12*, 98–105.

[13] [13a] J. Brickmann, *Localization of Hydrophobicity*, in: *Software Development in Chemistry* (Ed.: C. Jochum), GDCh Publ., Frankfurt, **1994**, pp. 139–156. – [13b] P. V. Pixner, W. Heiden, H. Merx, G. Moeckel, A. Möller, J. Brickmann, *J. Chem. Inf. Comput. Sci.* **1994**, *34*, 1309–1319.

[14] F. W. Lichtenthaler, *Zuckerindustrie* (Berlin) **1991**, *116*, 701–712.

[15] S. Immel, F. W. Lichtenthaler, *Liebigs Ann.* **1995**, 929–942.

[16] F. W. Lichtenthaler, S. Immel, *Tetrahedron Asymm.* **1994**, *5*, 2045–2060.

[17] F. W. Lichtenthaler, S. Immel, *Sucrose, Sucralose, and Fructose. Correlations between Hydrophobicity Potential Profiles and AH-B-X Assignments*, in: *Sweet Taste Chemoreception* (Eds.: M. Mathlouthi, J. A. Kanters, G. G. Birch), Elsevier Appl. Science, London/New York **1993**, pp. 21–53.

[18] Parts of this work are contained in a review: F. W. Lichtenthaler, S. Immel, *Computer Simulation of Chemical and Biological Properties of Sucrose, the Cyclodextrins, and Amylose*, in: *Intern. Sugar J.* **1995**, *97*, issue No. 1153, 12–22.

[19] [19a] *Cambridge Crystallographic Data File*, Version 5.09, **1995**, data sets with missing coordinates and more recent structure determinations have been included if atomic coordinates are provided within the written publications. – [19b] F. H. Allen, S. A. Bellard, M. D. Brice, B. A. Cartwright, A. Doubleday, H. Higgs, T. Hummelink, B. G. Hummelink-Peters, O. Kennard, W. D. S. Motherwell, J. R. Rodgers, D. G. Watson, *Acta Crystallogr., Sect. B*, **1979**, *35*, 2331–2339. – [19c] F. H. Allen, O. Kennard, R. Taylor, *Acc. Chem. Res.* **1983**, *16*, 146–153.

[20] The coordinates for the recent X-ray structure of the δ-CD hydrate[3] were neither deposited in the CCDF file, nor were they provided by the authors upon request; thus, a special procedure (cf. Experimental) was employed to reproduce the three-dimensional structure from the molecular plot given in the short communication[3].

[21] D. J. Heisterberg, *QTRFIT – Rigid Body Rotation and Fitting Program*. The Ohio Supercomputer Center, Columbus, Ohio, **1991**.

[22] [22a] D. Cremer, J. A. Pople, *J. Am. Chem. Soc.* **1975**, *97*, 1354–1358. – [22b] G. A. Jeffrey, J. H. Yates, *Carbohydr. Res.* **1979**, *74*, 319–322. – [22c] For six-membered rings three polar coordinate-type Cremer-Pople (CP) parameters Q, θ, and φ are necessary to describe the ring conformation. The puckering amplitude Q serves as a measure of the ring distortion only, being related to a atomic mean-square deviation from planarity. The angles θ (latitude) and φ (longitude) describe the ring conformation, e.g. $\theta \approx 54.7°/\phi \approx 60.0°$ corresponds to an E_1 geometry, while $\theta \approx 0.0°$ (in polar coordinates φ becomes meaningless for $\theta \rightarrow 0°$) is found for $^4C_1$ geometries.

[23] K. Harata, F. Hirayama, H. Arima, K. Uekama, T. Miyaji, *J. Chem. Soc., Perkin Trans. 2*, **1992**, 1159–1166.

[24] [24a] G. A. Jeffrey, W. Saenger, *Hydrogen Bonding in Biological Structures*, Springer Verlag, Berlin/New York, **1991**, Chapter 18: *OH···O Hydrogen Bonding in Crystal Structures of Cyclic and Linear Oligoamyloses: Cyclodextrins, Maltotriose, and Maltohexaose*, pp. 309–350; most notably pp. 315–318. – [24b] T. Steiner, W. Saenger, *Carbohydr. Res.* **1994**, *259*, 1–12.

[25] B. Casu, M. Reggiani, G. G. Gallo, A. Vigevani, *Tetrahedron* **1968**, *24*, 803–821.

[26] D. Rong, V. T. D'Souza, *Tetrahedron Lett.* **1990**, *31*, 4275–4278.

[27] G. A. Jeffrey, W. Saenger, *Hydrogen Bonding in Biological Struc-*

tures, Springer Verlag, Berlin/New York, **1991**, Chapter 13: *Hydrogen Bonding in Carbohydrates*, pp. 169–219; most notably pp. 183–185 and 198.
[28] F. W. Lichtenthaler, S. Immel, D. Martin, V. Müller, *Some Disaccharide-Derived Building Blocks of Potential Industrial Utility*, in: G. Descotes (Ed.), *Carbohydrates as Organic Raw Materials II*, VCH Publ., Weinheim/New York, **1993**, pp. 59–98; *Starch/Stärke* **1992**, *44*, 445–456.
[29] L. M. J. Kroon-Batenburg, J. Kroon, *Biopolymers* **1990**, *29*, 1243–1248.
[30] K. Bock, J. Ø. Duus, *J. Carbohydr. Chem.* **1994**, *13*, 513–543.
[31] This finding, corroborated by 98 X-ray structures of α-, β- and γ-CDs, is in contrast to conclusions reached by MM2 and AMBER molecular mechanics calculations, which generated asymmetric and highly distorted CD conformations as global minimum-energy structures. Thus, the contributions originating from hydrogen bond interactions have obviously been overestimated.
[32] B. Klar, B. E. Hingerty, W. Saenger, *Acta Crystallogr., Sect. B*, **1980**, *36*, 1154–1165.
[33] K. Lindner, W. Saenger, *Acta Crystallogr., Sect. B*, **1982**, *38*, 203–210.
[34] K. K. Chacko, W. Saenger, *J. Am. Chem. Soc.* **1981**, *103*, 1708–1715.
[35] M. J. Gidley, S. Bociek, *Carbohydr. Res.* **1988**, *183*, 126–130.
[36] J. J. Stezowski, J. M. MacLennan, *Am. Cryst. Assoc., Ser. 2*, **1980**, *7*, 24.
[37] T. Fujiwara, M. Yamazaki, Y. Tomizu, R. Tokuoka, K.-I. Tomita, T. Matsuo, H. Suga, W. Saenger, *Nippon Kagaku Kaishi (J. Chem. Soc. Jpn.)*, **1983**, 181–187.
[38] V. Zabel, W. Saenger, S. A. Mason, *J. Am. Chem. Soc.*, **1986**, *108*, 3664–3673.
[39] J. A. Ripmeester, *Supramol. Chem.* **1993**, *2*, 89–91.
[40] J. M. MacLennan, J. J. Stezowski, *Biochem. Biophys. Res. Commun.* **1980**, *92*, 926–932.
[41] K. Harata, *Bull. Chem. Soc. Jpn.* **1987**, *60*, 2763–2767.
[42] J. Ding, T. Steiner, V. Zabel, B. E. Hingerty, S. A. Mason, W. Saenger, *J. Am. Chem. Soc.* **1991**, *113*, 8081–8089.
[43] M. Fathallah, F. Fotiadu, C. Jaime, *J. Org. Chem.* **1994**, *59*, 1288–1293.
[44] [44a] F. M. Richards, *Ann. Rev. Biophys. Bioeng.* **1977**, *6*, 151–176; *Carlsberg. Res. Commun.* **1979**, *44*, 47–63. – [44b] M. L. Connolly, *J. Appl. Cryst.* **1983**, *16*, 548–558; *Science* **1983**, *221*, 709–713.
[45] B. Lee, F. M. Richards, *J. Mol. Biol.* **1971**, *55*, 379–400.
[46] Mathematical definition of the cavity dimensions and volumes: cross section cuts of the cyclodextrin contact surface with planes parallel to the mean plane of the macrocycle (*x*/*y*-plane) were calculated in steps of $\Delta z = 0.05$ Å. The topmost and bottommost contours, exhibiting separate inner and outer closed cyclic contours, were taken as cavity-limiting upper and lower boundaries.
[47] H. Nomura, S. Koda, K. Matsumoto, Y. Miyahara, *Stud. Phys. Theor. Chem.* **1983**, *27*, 151–163.
[48] K. Lindner, W. Saenger, *Carbohydr. Res.* **1982**, *107*, 7–16.
[49] K. Harata, *Bull. Chem. Soc. Jpn.* **1978**, *51*, 1644–1648.
[50] K. Harata, *Bull. Chem. Soc. Jpn.* **1979**, *52*, 2451–2459.
[51] See for example: K. Harata: [51a] *Bull. Chem. Soc. Jpn.* **1975**, *48*, 2409–2413. – [51b] *ibid.* **1976**, *49*, 2066–2072. – [51c] *ibid.* **1977**, *50*, 1416–1424. – [51d] *ibid.* **1980**, *53*, 2782–2786. – [51e] *ibid.* **1982**, *55*, 1367–1371.
[52] B. Klingert, G. Rihs, *J. Chem. Soc., Dalton Trans.* **1991**, 2749–2760.
[53] D. Mentzafos, I. M. Mavridis, G. LeBas, G. Tsoucaris, *Acta Crystallogr., Sect. B*, **1991**, *47*, 746–757.
[54] A. Rontoyianni, I. M. Mavridis, E. Hadjoudis, A. J. M. Duisenberg, *Carbohydr. Res.* **1994**, *252*, 19–32.
[55] I. M. Mavridis, E. Hadjoudis, *Carbohydr. Res.* **1992**, *229*, 1–15.
[56] K. Harata, *Bull. Chem. Soc. Jpn.* **1984**, *57*, 2596–2599.
[57] C. Jaime, J. Redondo, F. Sánchez-Ferrando, A. Virgili, *J. Mol. Struc.* **1991**, *248*, 317–329.
[58] J. A. Hamilton, *Carbohydr. Res.* **1985**, *142*, 21–37.
[59] S. Kamitori, K. Hirotsu, T. Higuchi, *J. Chem. Soc., Chem. Commun.* **1986**, 690–691.
[60] S. Kamitori, K. Hirotsu, T. Higuchi, *J. Am. Chem. Soc.* **1987**, *109*, 2409–2414; *Bull. Chem. Soc. Jpn.* **1988**, *61*, 3825–3830.
[61] H. Dodziuk, D. Sybilska, S. Miki, Z. Yoshida, J. Sitkowski, M. Asztemborska, A. Bielejewska, J. Kowalczyk, K. Duszczyk, L. Stefaniak, *Tetrahedron* **1994**, *50*, 3619–3626.
[62] Z.-I. Yoshida, H. Takekuma, S.-I. Takekuma, Y. Matsubara, *Angew. Chem.* **1994**, *106*, 1658–1660; *Angew. Chem. Int. Ed. Engl.* **1994**, *33*, 1597–1599.
[63] [63a] D. W. Griffiths, M. L. Bender, *Adv. Catal.* **1973**, *23*, 209–261.
[64] According to Webster's Dictionary, "in music, a final passage, which brings a composition to a definite, formal close".
[65] D. E. Koshland, Jr., *Angew. Chem.* **1994**, *106*, 2468–2471; *Angew. Chem. Int. Ed. Engl.* **1994**, *33*, 2408–2412.
[66] [66a] E. Fischer, *Ber. Dtsch. Chem. Ges.* **1894**, *27*, 2985–2993. – [66b] F. W. Lichtenthaler, *Angew. Chem.* **1994**, *106*, 2456–2467; *Angew. Chem. Int. Ed. Engl.* **1994**, *33*, 2364–2374.
[67] S. Immel, F. W. Lichtenthaler, *Liebigs Ann.*, in press.

[95264]